The Journal of Engineering and Exact Sciences – JCEC, Vol. 04 N. 01 (2018)
journal homepage: http://www.seer.ufv.br/seer/rbeq2/index.php/req2/index
doi: https://doi.org/10.18540/jcecvl4iss1pp0019-0027
OPEN ACCESS – ISSN: 2527-1075

NOVEL ZINC(II) DERIVATIVES OF PHENOL SCHIFF BASES: SYNTHESIS, CHARACTERISATION, CRYSTAL STRUCTURE AND ANTIMICROBIAL ACTIVITY

NOVOS DERIVADOS DE ZINCO(II) COM BASES DE SCHIFF FENÓLICAS: SÍNTESE, CARACTERIZAÇÃO, ESTRUTURA CRISTALINA E ATIVIDADE ANTIMICROBIANA

A. F. da S. SANTOS[1], M. C. de SOUZA[2], R. DINIZ[3], J. R. da S. MAIA[1*]

[1] Universidade Federal de Viçosa, Departamento de Química, Viçosa, MG, Brasil
[2] Universidade Federal de Juiz de Fora, Departamento de Química, Juiz de Fora, MG, Brasil
[3] Universidade Federal de Minas Gerais, Departamento de Química, Belo Horizonte, MG, Brasil

[*]*Corresponding author. Universidade Federal de Viçosa, Departamento de Química, Viçosa, MG, 36570-901, Brazil, Phone: +55 3138993058*
e-mail address: jrsmaia@outlook.com (J. R. da S. Maia).

A R T I C L E I N F O

Article history:
Received 2017-11-28
Accepted 2018-01-23
Available online 2018-02-28

p a l a v r a s - c h a v e
Bases de Schiff
Complexos de zinco(II)
Estrutura cristalina
Atividade antibacteriana

k e y w o r d s
Schiff bases
Zinc(II) complexes
Crystal structure
Antibacterial activity

A B S T R A C T

*Zinc(II)-Schiff base derivatives of general formula $[Zn(L)Cl]_n.xH_2O$ {n = 2; x = 1, L = 3-hmp (**1**), L = 4-hmp (**2**); x = 0, L = hmyp (**3**)} were synthesized by the condensation reaction of aminophenol with 2-hydroxybenzaldehyde. The Schiff bases in complex-**1**, **2** and **3** are bonded to the metal through the nitrogen and oxygen atoms. These complexes have dimeric structures with bridging oxygen atom. The metal is at the centre of a tetrahedron (**1** and **2**), and at a square pyramidal geometry (**3**), according to the X-ray diffraction analyses. They were characterized by IR, NMR (^1H, ^{13}C), molar conductivity, melting point and microanalyses. The bioassay of these Zn(II) derivatives on strains of S. aureus, B. subtillis, E. coli and S. typhimurium showed MICs between 60 and 520 μM. Complex-**2** showed the best antibacterial result with MIC of 65 μM against the Gram-positive bacteria.*

R E S U M O

*Compostos de zinco(II) com bases de Schiff de fórmula geral $[Zn(L)Cl]_n.xH_2O$ {n = 2; x = 1, L = 3-hmp (**1**), L = 4-hmp (**2**); x = 0, L = hmyp (**3**)} foram preparados mediante reação de condensação entre aminofenol com 2-hidroxibenzaldeído. As bases de Schiff nos complexos **1**, **2** e **3** formam ligações ao centro metálico via os átomos de nitrogênio e oxigênio. Estes compostos têm uma estrutura dimérica com átomos de oxigênio em ponte. O metal se encontra no centro de um tetraedro (**1** e **2**) e de uma pirâmide de base quadrada (**3**), segundo análise por difração de raios-X. Os compostos foram caracterizados por IR, RMN (^1H e ^{13}C), condutividade molar, pontos de fusão e microanálise. Ensaios biológicos em cepas de S. aureus, B. subtillis, E. coli e S. typhimurium mostraram MICs entre 60 e 520 μM. O complexo **2** mostrou o melhor resultado bactericida com MIC de 65 μM contra as bactérias Gram-positivas.*

1. INTRODUCTION

Novel therapeutic agents have been calling attention in the last decades to suppress the resistance of microorganisms to commercial fungicides and bactericides. Schiff bases and its coordination compounds are within the class of substances that can be considered as therapeutic agents because of their bactericide, fungicide, antiviral and antitumoral activity (Creaven *et al*., 2010; Singh *et al*., 2010; Qiao *et al*., 2011; Kursunlu *et al*., 2013).

Nowadays metal-based compounds derivatives of Schiff bases might be recognized as a forthcoming medicine to be used in the treatment of human diseases because of the great activity of these compounds on microorganisms and their property of binding DNA. Some examples are copper(II), nickel(II) and cobalt(II) derivatives of 1,2,4-triazole Schiff bases which showed MICs in the range of 10 to 100 $\mu g\ mL^{-1}$ on several microorganisms. Chelates of zinc(II)-Schiff base derivatives of 4-morpholinoaniline also showed great antimicrobial activity against *P. aerugonisa* and *C. albicans* in comparison to their corresponding Schiff base. The binding properties of Zn(II)-heterocyclic Schiff base derivatives to CT-DNA are also reported in the literature (Bagihalli *et al*., 2009; Arjmand *et al*., 2011; Dhahagani *et al*., 2014).

The stereochemistry of Schiff bases regarding the imine bond let these compounds to be acknowledged as a mixture of E and Z isomers in solid state. Apparently, the E isomer is thermodynamically stable in solution. Nevertheless, the interconversion of the Z isomer into the E one is known from zinc(II)-Schiff base compounds where the E isomer seem to be the favoured conformation to bind metals in coordination chemistry (Wen *et al*., 2012). In this work, the data collected show that the E isomer have coordinated to the metal only. No evidence for the coordination of the Z isomer was detected.

Continuing with our research program on biological activity of coordination compounds, this work reports the synthesis, spectroscopic characterisation, and antimicrobial activity of zinc(II)-Schiff bases derivatives on pathogenic microorganisms. These compounds have been bioassayed for Gram-positive and Gram-negative pathogens with promising results. The bioassay data showed MIC values within the range reported in the literature for transition metal-Schiff base derivatives.

2. MATERIALS AND METHODS

Reagents and solvents were purchased from Sigma-Aldrich, Vetec or FMaia companies and were used without prior purification. The microanalyses were gotten from a Perkin Elmer 200 CHN Elemental Analyser. The molar conductivity of the complexes was carried out using a Conductivity Jenway Meter 4010 in methanol. The infrared spectra were recorded in CsI pellets using a Perkin Elmer FT-IR 1000. The multinuclear NMR (^1H and ^{13}C) spectra was obtained by means of a Varian Mercury 300 MHz in $CDCl_3$ and DMSO-d_6. Single crystal X-ray data were collected at room temperature by an Oxford GEMINI A – Ultra diffractometer with MoKα (λ = 0.71073 Å). Data reduction and cell refinement were analysed by the CrysAlis RED program (Oxford diffraction Ltd – Version 1.171.32.38 program) (Crysalisred, 2008). The crystal structure was resolved and refined by SHELXL-97 (Sheldrick, 1997). Multiscan absorption corrections were applied according to the method previously reported in the literature (Blessing, 1995). The non-hydrogen atoms were correlated with anisotropic displacement parameters at 1.2 Ueq of their corresponding carbon atoms. A rigid model with C–H distances of 0.93 Å for aromatic and 0.96 Å for methylene groups defined the hydrogen atoms. The structures were drawn by ORTEP-3 for Windows and Mercury computing programs (Farrugia, 1997; Macrae *et al*., 2006). The minimum inhibitory concentration (MIC) was determined by broth microdilution method using a spectrophotometer Eliza (600 nm) and microplates BioRad model 3550-UV, USA

2.1. Synthesis of the Schiff Bases

The synthesis and characterisation by infrared spectroscopy of *3-*, *4-hmp* and *hmyp* Schiff bases are reported in previous work by our research group on cooper(II) derivatives (Santos *et al*., 2016). However, the hydrogen and carbon 13 NMR data of these Schiff bases were not reported before and are presented herein for comparison to the zinc(II) derivatives.

(E)-2-(((3-hydroxyphenyl)imino)methyl)phenol(*3-hmp*) ^1H NMR (DMSO-d_6, 300 MHz, δ): 10.24 (s, C13-OH); 9.67 (s, C1-OH); 8.88 (s, HC7=N); 7.63 (d, J = 7.0 Hz, C9-H); 7.39 (t, C11-H); 7.23 (t, J = 7.9 Hz, C3-H); 6.94 (t, J = 7.9 Hz, C10-H, C12-H); 6.82 (d, J = 8.4 Hz, C4-H); 6.76 (s, C6-H); 6.72 (d, J = 8.0 Hz, C2-H). ^{13}C NMR (DMSO-d_6, 75 MHz, δ): 163.6 (C13); 160.7 (C7); 158.7 (C1); 149.6 (C5); 133.6 (C11); 133.0 (C9); 130.6 (C3); 119.6 (C10); 119.5 (C8); 116.9 (C12); 114.5 (C4); 112.4 (C2); 108.5 (C6).

(E)-2-(((4-hydroxyphenyl)imino)methyl)phenol(*4-hmp*) ^1H NMR (DMSO-d_6, 300 MHz, δ): 13.44 (s, C13-OH); 9.71 (s, C1-OH); 8.88 (s, HC7=N); 7.57 (d, J = 7.5 Hz, C9-H); 7.32 (t, C11-H); 6.93 (t, J = 7.6 Hz, C3-H, C10-H); 6.83 (d, J = 8.7 Hz, C2-H, C12-H). ^{13}C NMR (DMSO-d_6, 75 MHz, δ): 160.6 (C13); 160.5 (C7); 157.3 (C1); 139.5 (C4); 132.9 (C11); 132.6 (C9); 123.1 (C3, C5); 119.8 (C10); 119.4 (C8); 116.8 (C12); 116.3 (C2, C6).

(E)-2-(((1-hydroxy-2-methylpropan-2-yl)imino)methyl)phenol(*hmyp*) ^1H NMR ($CDCl_3$, 300 MHz, δ): 9.87 (s, C11-OH); 8.32 (s, HC5=N); 7.26 (dd, J =7.7 Hz, C7-H, C9-H); 6.89 (d, J = 8.3 Hz, C10-H); 6.82 (t, J = 7.4 Hz, C8-H); 3.56 (s, CH_2);1.30 (s, C2, C4, $2CH_3$); 1.16 (s, C1-OH);. ^{13}C NMR ($CDCl_3$, 75 MHz, δ): 162.6 (C11); 162.2 (C5); 132.5 (C9); 131.7 (C7); 118.4 (C6); 118.1 (C8); 117.5 (C10); 70.9 (C1); 60.8 (C3); 23.5 (C2, C4).

2.2. Synthesis of the Zn(II)-Schiff base Derivatives

The synthesis of these compounds followed the procedure described in the literature with slight modifications (Arjmand *et al*., 2011). Despite the stoichiometry used between the metal precursor and the appropriate Schiff base,

only 1:1 (M:L) products have been achieved. The zinc(II) compounds were prepared according to the general procedure: to a bottom flask of 125 mL, 1.423 mmol of Zn(II) chloride and 1.450 mmol of the appropriate Schiff base were dissolved in ethanol (30 mL). The mixture was heated at 70 °C, kept under reflux and stirring for 4 h. After reducing the volume of the mixture until dryness, the residue was dissolved in chloroform (30 mL). Subsequently, the chloroform was removed under reduced pressure and a solid separated which was washed with hexane before storing in desiccators.

[Zn(*3-hmp*)Cl]$_2$.H_2O (**1**): Color: brown yellowish; Yield of 0.460 g (87 %). Mp (°C): 119 d. Elemental analysis required for $C_{26}H_{22}N_2O_5Zn_2Cl_2$: C, 48.48; H, 3.44; N, 4.35. found: C, 48.36; H, 3.64; N, 4.40. Molar conductivity (ΩM): 0.08 ohm^{-1} mol^{-1} cm^2; IR (Nujol/CsI, νmáx/cm^{-1}): 3362 ν(OH); 1638 ν(C=N); 587 ν(Zn-O); 429 ν(Zn-N); 299, 288 ν(Zn-Cl); ^{1}H NMR (DMSO-d_6, 300 MHz, δ): 10.26, 10.72 (s, broad, C13-OH); 9.67 (s, broad, C1-OH); 8.91 (s, HC7=N); 7.65 - 6.71 (Ph, C-H). ^{13}C NMR (DMSO-d_6, 75 MHz, δ): 163.3, 163.1 (C13); 160.3 (C7); 158.3 (C1); 149.1 (C5); 133.3 (C11); 132.6 (C9); 130.2 (C3); 119.4 (C10); 119.1 (C8); 117.2 (C12); 114.1 (C4); 112.0 (C2); 108.1 (C6).

[Zn(*4-hmp*)Cl]$_2$.H_2O (**2**): Color: green olive; Yield of 0.389 g (74 %); Mp (°C): 130 d. Elemental analysis required for $C_{26}H_{22}N_2O_5Zn_2Cl_2$: C, 48.48; H, 3.44; N, 4.35. found: C, 48.96; H, 4.01; N, 4.35. Molar conductivity (ΩM): 0.21 ohm^{-1} mol^{-1} cm^2; IR (Nujol/CsI, νmáx/cm^{-1}): 3344 ν(OH); 1637 ν(C=N); 586 ν(Zn-O); 490 ν(Zn-N); 309, 294 ν(Zn-Cl). ^{1}H NMR (DMSO-d6, 300 MHz, δ): 10.26, 10.72 (s, broad, C13-OH); 9.74 (s, broad, C1-OH); 8.93 (s, HC7=N); 7.62 - 6.90 (Ph, C-H). ^{13}C NMR (DMSO-d6, 75 MHz, δ): 160.1 (C13); 157.2 (C7); 157.0 (C1); 138.8 (C4); 132.7 (C11); 132.2 (C9); 124.3 (C3, C5); 119.2 (C8); 119.0 (C10); 116.4 (C12); 115.9 (C2, C6).

[Zn(*hmyp*)Cl]$_2$ (**3**): Color: light yellow; Yield of 0.303 g (44%); Mp (°C): 279 d. Elemental analysis required for $C_{22}H_{28}Cl_2N_2O_4Zn_2$: C, 45.08; H, 4.81; N, 4.78. found: C, 45.43; H, 4.94; N, 4.80. Molar conductivity (ΩM): 0.04 ohm^{-1} mol^{-1} cm^2; IR (Nujol/CsI, νmáx/cm^{-1}): 3378 ν(OH); 1628 ν(C=N); 540 ν(Zn-O); 509 ν(Zn-N); 288, 278 ν(Zn-Cl). ^{1}H NMR (DMSO-d6, 300 MHz, δ): 8.35 (d, J = 8.6 Hz, HC5=N); 7.26 - 6.45 (Ph, C-H); 3.42 (s, CH_2); 1.28 (s, C2, C4, 2CH_3); 1.22 (s, C1-OH); RMN de ^{13}C (DMSO-d6, 75 MHz, δ): 170.4 - 170.2 (C11); 168.5 - 168.0 (C5); 137.1 - 136.8 (C9); 134.3 (C7); 122.6 (C6); 118.9 (C8); 113.3 (C10); 68.8 - 68.6 (C1); 62.2 - 61.7 (C3); 24.9 (C2, C4).

2.3. Minimum Inhibitory Concentration (MIC)

The minimum inhibitory concentration (MIC) was determined by the broth microdilution technique using microplates of 96 wells according to the methodology described in the literature (NCCLS, 2002; 2003; Zacchino e Gupta, 2007). The concentration of the standard solution was 1000 µg mL^{-1} which was obtained by dissolving 1.0 mg of the substance test in a mixture of DMSO (250 µL) with sterile water (750 µL). Subsequent aliquots for the bioassay screening were prepared diluting the standard solution to a range of concentrations in the range of 1950 to 0.5 µM (336 to 0.2 µg mL^{-1}). Each of the bacteria strain were grown in 3.0 mL of Luria Bertani (LB) medium at 37 °C under stirring until an optical density (OD) between 0.08 and 0.10 being achieved, equivalent to 1.0 to 2.0 x 10^8 colony-forming unit (CFU) mL^{-1}. Subsequently, 100 µL (5.0 x 10^4 CFU) of LB from each bacterial strain was added to 50 µL of the zinc(II) substance test. The resultant mixture was transferred to microplates for incubation throughout 24 h and scanned using a spectrometer ELISA at 600 nm. The experiment was finished in duplicate considering the standard deviation. The negative control was DMSO and the positive ones were *Amoxicillin* and *Norfloxacin*. The strains of bacteria used in the bioassay of the zinc(II)-Schiff base derivatives were *Staphylococcus aureus* (ATCC33591), *Bacillus subtilis* (ATCC 23858), *Escherichia coli* (ATCC 29214) and *Salmonella typhimurium* (ATCC 14028).

3. RESULTS AND DISCUSSION

Three Schiff bases were synthesized for complexation with zinc(II) chloride. The Schiff bases prepared are ambidentate ligands which can make covalent bonds to the metal through atoms of nitrogen, oxygen or both. The *3-hmp* and *4-hmp* are isomers which diverge from each other by the *ortho* and para position of the hydroxyl group at the phenyl ring bonded to the nitrogen atom of the imine moiety. The conductimetric measurements of the Zn(II)-Schiff base derivatives in methanol showed these compound as non-electrolytes.

3.1. Infrared Spectroscopy

The Schiff base ligands showed a typical infrared band in the region of 1623 cm^{-1} related to the stretching mode of the imine bond which is very characteristic of this class of compounds (Abdallah *et al*., 2009; Abdel-Rahman *et al*., 2013). Broad vibrational bands were exhibited in the region of 3289 cm^{-1} which are related to the stretching mode of the hydroxyl moiety bonded to the phenyl groups (Tavman *et al*., 2010). The molecular structures of these Schiff bases are presented in Figure 1. Upon coordination broad bands were also revealed in the region of 3412 cm^{-1}. These bands were correlated to both hydrogen bonding in solid state and vibrational modes of water molecules within the crystal array of the complexes (Nakamoto, 1997; Tavman *et al*., 2010). The stretching mode related to the imine moiety of these Schiff bases has shifted towards high frequency to the region of 1634 cm^{-1}, confirming the formation of a metal-imine bond (Abdallah *et al*., 2009; Abdel-Rahman *et al*., 2013; Kursunlu *et al*., 2013).

New bands in the region of 476 cm^{-1} and 571 cm^{-1} were assigned to the metal-nitrogen and metal-oxygen bonds respectively (Prakash *et al*., 2010; Singh and Singh, 2012). The infrared region of the metal-oxygen bonds in complex-**1**, **2** and **3** are in the range expected for bridging metal-oxygen bonds. These bonds are usually stronger in comparison to the terminal ones. For instance, the structure of dimeric and monomeric palladium compounds, determined by X-ray diffraction analysis, showed shortened bond length of the bridging metal-oxygen bonds in the dimer relative to the terminal ones in the monomer (Sakaguchi *et al*., 2008). Thus, the metal-oxygen bond strength in these palladium compounds corroborate with the infrared band for the same bond type of the Zn(II)-Schiff base derivatives. Chelated dimeric and monomeric compounds

of transition metals such as Co(II), Ni(II), Cu(II), Pd(II) and Mn(II) derivatives of Schiff bases also showed stretching modes of terminal metal-oxygen bonds in the region of 533 cm^{-1} (Geeta *et al.*, 2010; Singh *et al.*, 2017).

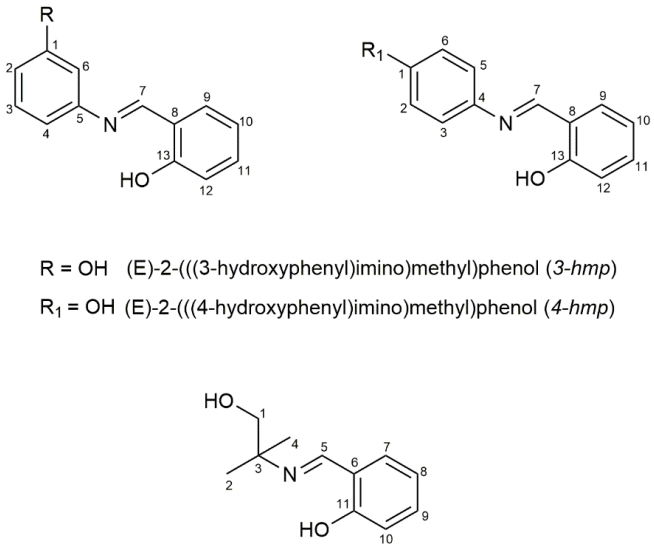

Figure 1 - Molecular structure of the Schiff bases.

The infrared spectra of both complex-**1** and **2** suggest that these compounds followed an equivalent reaction pathway. The slight differences in vibrational stretching of the metal-nitrogen bond between them may be caused by the resonance properties of the free hydroxyl groups at the *ortho* and *para* position from the phenyl moiety in the *3*- and *4*-hmp ligands. Furthermore, the proximate vibrational stretching of the metal-oxygen bond in these complexes is evidence that both have comparable geometrical arrangements. Complex-**1** and **2** have the ligands bonded to the metal through a bidentate coordination mode instead of a tridentate one as in complex-**3**. Higher coordination number is not conceivable for the former two compounds because the *3*- and *4-hmp* have the *ortho* and *para* hydroxyl group coplanar with the phenyl ring in contrast with complex-**3** which has a hydroxyl group bonded to the flexible aliphatic chain of *hmyp*.

Two metal-chlorine absorptions were observed in the range of 275 to 310 cm^{-1} within the spectra of these zinc(II) complexes. The difference between these two infrared bands is around 12 cm^{-1} which arises the hypothesis that all chlorine atoms have the same characteristic regarding the coordination mode. Thus, the chlorine atoms in complex-**1** and **2** are bonded to the metal in a monodentate coordination mode like those in complex-**3** showed in Figure 3. However, the metal is most likely at the centre of a distorted tetrahedral arrangement in solid state as showed in Figure 2.

3.2. NMR Spectroscopy

The hydrogen NMR showed singlet signals assigned to the imine moiety (N=C7-H) of the free *3*- and *4-hmp* in DMSO at δ 8.88, and at δ 8.32 for *hmyp* (N=C5-H) in $CDCl_3$. However, in the spectra of the complexes, the signal corresponding to the imine moiety of complex-**3** split into a doublet at δ 8.35 most likely related to a structural asymmetry of the N=C5-H group in solution which is linked to the geometric arrangement of this complex. These signals shifted by approximately δ 0.03 downfield for the zinc(II) derivatives of *3*- and *4-hmp* and upfield to similar extent for the *hmyp* derivative, confirming the coordination through the imine group from these Schiff bases regardless of the solvent effect. The NMR (^{1}H and ^{13}C) of complex-**3** was obtained in DMSO because this compound was not soluble in $CDCl_3$.

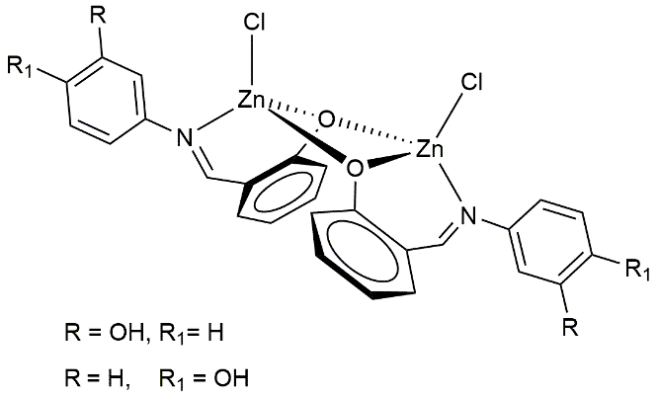

Figure 2 - Proposed dimeric homo-bimetallic tetrahedral structure of complex-1 and 2.

The resonance signals at δ 10.24 and 13.44 (C13-OH) of the free *3*- and *4-hmp*, and the one at δ 9.87 (C11-OH) of *hmyp* in $CDCl_3$ are correlated to a strong intramolecular hydrogen bonding between the nitrogen atom of the imine moiety and the vicinal phenolic hydroxyl group (Tavman *et al.*, 2010). The hydroxyl group at the aliphatic chain of the free hmyp resonates at δ 1.16 (C1-OH) and the ones at the *ortho* and *para* position on the phenyl ring of *3*- and *4-hm*p at δ 9.67 and 9.71 (C1-OH) respectively. The signal of these hydroxyl groups did not shift significantly upon coordination nor the one of the *hmyp* aliphatic chain, despite the solvent effect. However, the *ortho* and *para* hydroxyl signals of the two isomers, *3*- and *4-hmp*, were broad in the spectral region of δ 9.70 of the equivalent complexes. Two broad signals at δ 10.26 and 10.72 (C13-OH) also appeared in the spectrum of both complex-**1** and **2**. In comparison to the free ligands, these signals shifted in an average of δ 0.5 downfield for the *3-hmp*, and of δ 2.95 upfield for the *4-hmp*. On the other hand, the phenolic hydroxyl signal at δ 9.87 (C11-OH) from the *hmyp* disappeared in complex-**3**, confirming the formation of metal-oxygen bonds after releasing hydrochloric acid in the medium.

The outcome of the broad signals in the region of δ 10.49 and 9.70 was observed only for complex-**1** and **2**. The *3*- and *4-hmp* have structural features that restricts the formation of a metal-hydroxyl bond in contrast with the aliphatic chain in complex-**3** showed in Figure 3; these broad signals are most likely related to the formation of hydrogen bonding (Tavman *et al.*, 2010). Considering that, these signals are the result of an intermolecular hydrogen bonding between the water molecules and the bridging metal-oxygen bonds from the tetrahedral arrangement in Figure 2. Nevertheless, hydrogen bonding is also possible through the hydroxyl groups at the *ortho* and *para* position on the phenyl ring of the Schiff bases.

The carbon 13 NMR showed signals associated with the imine moiety at δ 160.7, 160.5 (C7) for the *3*- and *4-hmp*

separately, and δ 162.2 (C5) for *hmyp*. The signals of complex-1 and **2** shifted to δ 160.3 and 157.2, and two signals at δ 168.5 and 168.0 (C5) were revealed for complex-**3** in DMSO, owing to asymmetry of the metal-nitrogen bond within the magnetic environment.

The same was noticed in the chemical shift of the aromatic carbon atoms bonded to the phenolic hydroxyl group in the complexes. For the free *3-hmp*, the chemical shift of the carbon atom (C13) was at δ 163.6 and for *4-hmp* at 160.6. The previous signal of complex-**1** split up into two ones and shifted slightly upfield to δ 163.3 and 163.1 most likely because of magnetic asymmetry. The signal at δ 160.6 of complex-**2** shifted to 160.1 without splitting. The spectrum of complex-**3** also showed fragmented signals related to the phenyl carbon atom (C11) bonded to the phenolic bridging oxygen atoms from *hmyp*. For this complex, the split signals at δ 170.4 and 170.2 in DMSO have an obvious downfield chemical shift in comparison to those of complex-**1** and **2** in the same solvente. Consequently, the observed chemical shift corresponds to a deshielding effect in complex-**3**, and a shielding one in complex-**1** and **2**.

The shielding and deshielding of these aromatic carbon atoms (C13 and C11) can be envisaged accounting for the geometrical features of these complexes. In solution, complex-**3** may be represented by an interconversion between dimers having two distinct structural arrangements: a distorted bipyramid trigonal and a distorted square pyramidal geometry.

Both geometrical arrangements have the same hybridization of the Zn(II) ion (sp^3d). The *d* orbitals of the metal that do not participate in the Zn(II) hybridization might line up with the perpendicular *p* orbitals to the hybrid sp^2 ones of the bridging oxygen atoms. Presumably, this orbital configuration supports electron delocalization over the bridging metal-oxygen ring. The formation of a π (*d-p*) covalent bond in complex-**3** is corroborated by the bond angles of O2-Zn-O2i (76.8°) and Zn-O2-Zn (102.7°) from its crystal structure showed in Figure 3.

On the other hand, the proposed tetrahedral arrangement for complex-**1** and **2** does not involve *d* orbitals in the hybridization of the Zn(II) ion (sp^3). Consequently, the formation of a π (*d-p*) bond over the metal bridging-oxygen atoms is insignificant, supporting the observable shielding of the carbon atoms in connection to the tetrahedral arrangement of these complexes.

3.3. Crystallography

The structure of Complex-**3** has been determined by X-ray diffraction analysis. This complex crystalizes in orthorhombic system and space group Pbcn. The crystallographic data and selected bond lengths and angles are listed in Table 1 and 2, respectively. The X-ray analyses indicate that the dimeric structure in Figure 3b was obtained by the 2-fold screw axis operation from the asymmetric unit showed in Figure 3a.

The crystal structure of complex-**3** showed bond angles surrounding the metal centre that suggest the formation of a distorted bipyramid trigonal or a square pyramidal geometry. However, the geometry index (τ) of complex-**3** is 0.32, which indicates that the zinc(II) ions are coordinated in a distorted square pyramidal geometry (Addison *et al.*, 1984). The ligands are asymmetrically coordinated to the metal in a tridentate coordination mode corroborated by the Zn-O1, Zn-O2, ZnO2i, Zn-N1 and Zn-Cl bond distances showed in Table 2.

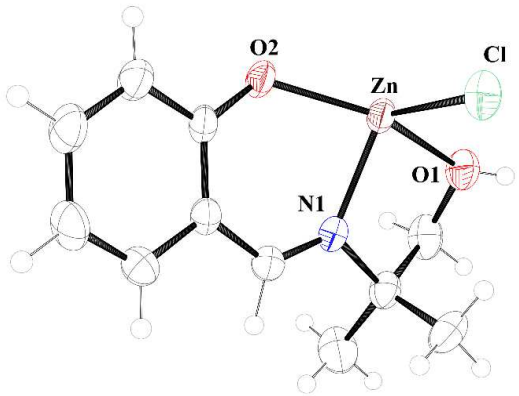

(a)

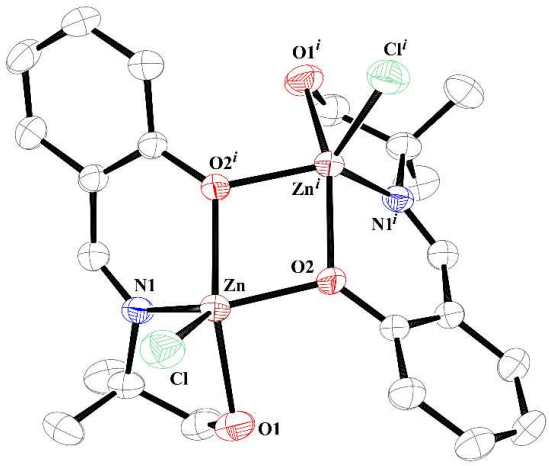

(b)

Figure 3 - ORTEP representation of the asymmetric unit (a) and the dimeric one of complex-3 (b). Symmetry code (i): 1 - x, y, 1.5 - z.

In addition, the chlorine atoms bonded to the metal are coplanar in *cis* position. Other dimeric structures of zinc(II)-Schiff base derivatives having the metal penta- and hexacoordinated are reported in the literature (Wen *et al.*, 2012). The crystal structure of complex-**3** shows a weak hydrogen bonding of the type O1-H1···Clii {2.530 Å} as well as O1···Clii {3.201(1) Å} which contributes for the crystal packing of this compound. The unit cell is displayed in Figure 4a. The hydrogen bonding arrangement gives rise to a one-dimensional network along *c* crystallographic axis in Figure 4b, and the two-dimensional network is obtained by weak interactions of CH···Cl along *a* axis in Figure 4c.

Table 1 - Crystal data and refinement parameters of complex-3.

Formula	$C_{22}H_{28}Cl_2N_2O_4Zn_2$
Molecular weight (g.mol^{-1})	586.10
Crystal system	Orthorhombic
Space group	Pbcn
a (Å)	14.1392(3)
b (Å)	9.7133(2)
c (Å)	17.9556(3)
α = β = γ (°)	90.00
Volume (Å3)	2463.35(8)
Z	4
Dcalc.(g.cm^{-3})	1.581
Radiation (KαMo)	λ = 0.71073 Å
Θ limits (°)	2.268–29.524
Reflections collected / independent	40541 / 3315
Reflections observed [$F^2_{obs}>2\sigma_{(Fobs)}$]	2786
Parameters	145
R indices [$F^2_{obs}>2\sigma_{(Fobs)}$]	R1 = 0.0247 wR2 = 0.0600
R indices for all data	R1 = 0.0346 wR2 = 0.0658 S = 1.096

Table 2 - Selected bond lengths and bond angles of complex-3.

Bond lengths (Å)			
Zn-O1	2.203(1)	N1-C7	1.279(2)
Zn-O2	2.048(1)	N1-C8	1.487(2)
Zn-O2i	1.992(1)	O1-C9	1.418(2)
Zn-Cl	2.258(5)	O2-C2	1.329(2)
Zn-N1	2.064(1)		
Bond angles (°)			
Cl-Zn-O1	97.18(4)	O2-Zn-O2i	76.85(5)
Cl-Zn-O2	112.69(4)	O2i-Zn-N1	130.84(5)
Cl-Zn-O2i	114.12(4)	Zn-O2-Zn	102.73(5)
Cl-Zn-N1	115.01(4)	C7-N1-Zn	124.22(2)
O1-Zn-N1	78.60(5)	C8-N1-Zn	116.06(2)
O1-Zn-O2	150.02(5)	C9-O1-Zn	108.2(1)
O1-Zn-O2i	93.69(5)	C2-O2-Zn	124.7(1)
O2-Zn-N1	86.24(5)	C2-O2i-Zn	130.6(1)
Torsion angles (°)			
C1-C7-C1-C8	9.45	N1-C8-C9-O1	49.5
C7-N1-C8-C1	-83.8	C8-C9-O1-Zn	-41.3
C7-N1-C8-C1	40.2	C1-C2-O2-Zn	-31.7
C7-N1-C8-C9	157.6	Cl-Zn-O2-Zni	118.0
C7-C1-C2-O2	-0.27	Cl-Zn-O2i-Zni	116.2

Hydrogen bonding interactions				
D H A	D-H (Å)	H· A (Å)	D··A (Å)	D-H· A (°)
O1-H1··Cl^{ii}	0.730	2.530	3.201(1)	154.0

Supplementary data: X-ray crystallographic data of complex-**3** was deposited with the Cambridge Crystallographic Data Centre (CCDC), 12 Union Road, Cambridge CB2 1EZ, UK; Fax: +44(0)1233 336033), and it can be requested free of charge at www.ccdc.cam.ac.uk/conts/retrieving.html or by the e-mail: deposit@ccdc.cam.ac.uk, quote CCDC 1553418.

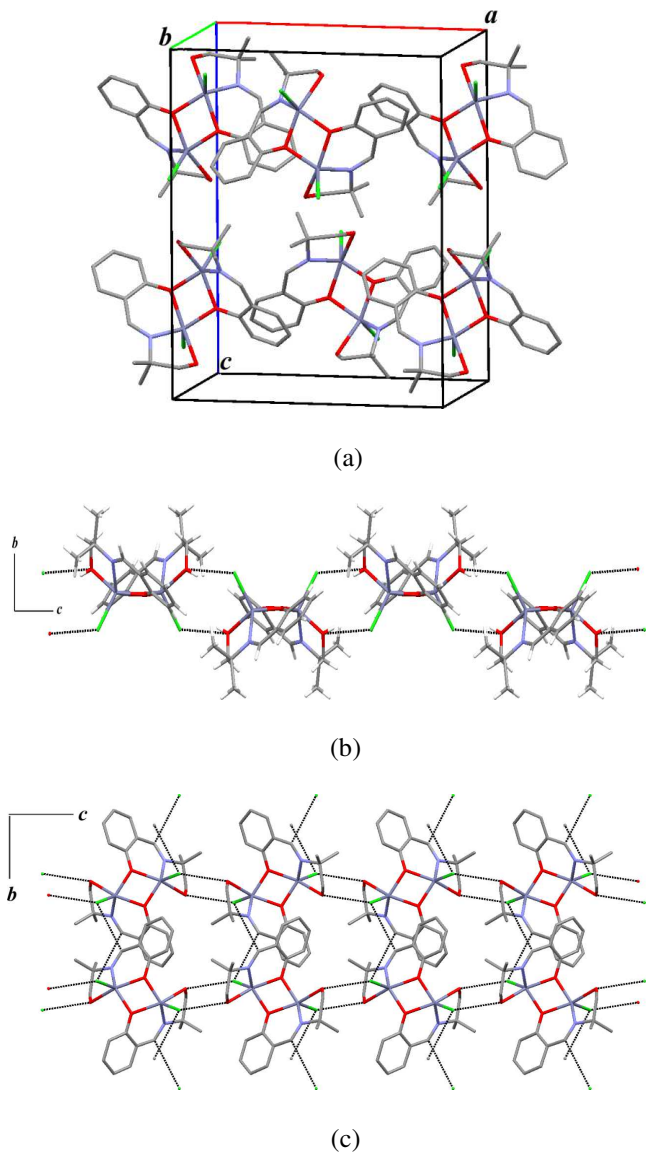

Figure 4 – ORTEP Representation of the crystal packing of complex-3: (a) hydrogen and oxygen interactions, (b) intermolecular interaction of the type CH…Cl and (c) the crystal packing along the axis *a*, *b* and *c*. symmetry code (i): 1 - x, y, 1,5 – z e (ii): 1 - x, -y, 2 –z.

3.4. Bacterial Activity

Antimicrobial effect of zinc(II) compounds are illustrated in the literature for several ligand types including Schiff bases with various substituent groups. The chelating properties of coordination compounds is acknowledged to increase lipophilicity of complexes. This property enhances the penetration across the lipid membrane of the microorganisms, blocking the metal to bind enzymes (Alaghaz *et al.*, 2015; Hu *et al.*, 2016).

A wide range of MICs associated with Zn(II)-Schiff base derivatives is reported in the literature. For instance, a chelated monomer of Zn(II)-2-bromo-4-chloro-6-[(2-morpholin-4-ylethylimino)methyl]phenol revealed MIC values of 2.0 µg mL^{-1} for *S. aureus* and 8.0 µg mL^{-1} for *E. coli* (Hu *et*

al., 2016). The Zn(II)-salicylaldimine derivatives presented MICs in the range of 50 to 500 µg mL^{-1} on *S aureus* where the absence of lipophilicity decreased the activity of some compounds bioassayed (Kaczmarek *et al*., 2009).

Monomeric chelated tetrahedral Zn(II)-Schiff base derivatives of 3-bromosalicylaldehyde and 5-methoxy-2-[(3-methylaminopropylimino)methyl]phenol showed MIC values in the range of 4.0 to 13.0 µg mL^{-1} on *S. aureus* and *E. coli* (Xue *et al*., 2011; Xue *et al*., 2013). However, other tetracoordinated Zn(II)-Schiff base derivatives revealed a zone of inhibition growth in the range of 625 to 2500 µg / disk (0.625 to 2.5 mg / disk) on *S. aureus* and *E.coli* contrasting with the chelated octahedral Zn(II)-2-((E)-(2-methoxyphenylimino)methyl)-4-bromophenol; the latter showed MIC of 150 to 125 µg mL^{-1} for the same microorganisms (Adly *et al*., 2013; Galini *et al*., 2017; Taghizadeh *et al*., 2017).

The Zinc(II)-Schiff base complexes prepared in this work have been tested on the Gram-positive *S. aureus* and *B. subtillis* as well as the Gram-negative *E. coli* and *S. typhimurium* to evaluate their potential to become antimicrobial drugs. The resultant bioassay data are showed in Table 3. Nevertheless, these ligands were less active in comparison to the antibiotics *Amoxicillin* and *Norfloxacin*.

Among the compounds bioassayed, complex-**1**, **3** and zinc(II) chloride dihydrate have shown moderate activity compared to complex-**2** which presented the best result on *S. aureus* and *B. subtillis*. The synergistic effect between *3-hmp* and the Zn(II) ion can be perceived by the activity of complex-**1**. This complex also showed great activity on the microorganisms tested in comparison to zinc(II) chloride. However, the synergistic effect between the *4-hmp* and the Zn(II) ion was superior with regards to the MIC of complex-**2** on *S. aureus* and *B. subtillis*. It seems that the *para* hydroxyl group from *4-hmp* might have an influence on the bactericide effect of this compound regarding its electron-donor property

The complex-**2** and **3** appear to be selective towards the Gram-positive microorganisms. The bioassay results of these complexes suggest that the dimeric tetrahedral arrangement of the former overcome the structural interconversion of the latter in solution concerning the biochemical interaction with the microorganisms.

All these zinc(II) complexes in Table 3 have considerable lipophilic effect by chelation except zinc(II) chloride. The biological activity of this compound, showed by its MIC datum, is probably related to the absence of chelation between the chloride and the Zn(II) ion. Even though the structure of *Amoxicillin* and *Norfloxacin* have both common substituent groups with the zinc(II) complexes, a mechanism of action could not be envisaged based on these common chemical features.

Table 3 – MIC* of the Zinc(II)-Schiff base complexes against Gram-positive and Gram-negative microorganisms

Compound	SA	BS	EC	ET
3-hmp	*na*	*na*	*na*	*na*
4-hmp	196	389		
	(42)	(83)	*na*	*na*
hmyp			1723	
	na	*na*	(333)	*na*
(**1**)	257	257	516	516
	(166)	(166)	(333)	(333)
(**2**)	65	65		
	(42)	(42)	*na*	*na*
(**3**)	283	283		
	(166)	(166)	*na*	*na*
Amox	13.6	0.5		
	(5)	(0.2)	*na*	*na*
Norflox	15.6	4.1	1.8	4.1
	(5)	(1.3)	(0.6)	(1.3)
$ZnCl_2.2X$	481	481	1932	1932
	(83)	(83)	(333)	(333)

Note: *Minimum Inhibitory Concentration (MIC) - µM (µg mL^{-1}); *na* – compound inactive at the highest concentration used in the experiment; SA – *S. aureus*; BS – *B. subtillis*; EC – *E. coli*; ST – *S. typhimurium*; (**1**) - $[Zn(3\text{-}hmp)Cl]_2.H_2O$; (**2**) - $[Zn(4\text{-}hmp)Cl]_2.H_2O$; (**3**) - $[Zn(hmyp)Cl]_2$; Amox – *Amoxicilin*; Norflox – *Norfloxac*in; 2X – $2H_2O$.

4. CONCLUSION

The biochemical interaction of these complexes with the microorganisms seems to be linked to several properties. For instance, the synergistic effect between the metal ion and the Schiff bases, the coordination chemistry features, the stereochemistry of the free hydroxyl groups, the lipophilic effect upon coordination, and the distinct double cell wall of the Gram-negative microorganisms.

The dimeric tetrahedral compound, complex-**2**, showed better MIC (µM) in comparison to complex-**1** and **3**. This suggests that the dimeric tetrahedral arrangement in combination with the *para* position of the hydroxyl group from the *4-hmp* ligand might enhances the antimicrobial activity of this compound, although the mechanism of action is still unknown.

The bioassay data of these zinc(II)-Schiff base derivatives shows that these compounds can eventually be useful in the chemical composition of pharmaceutical medicines for the treatment of human illnesses

ACKNOWLEDGEMENTS

The authors are grateful to the Brazilian Agencies FAPEMIG, CNPq and CAPES for financial support.

REFERENCES

ABDALLAH, S. M. et al. Spectroscopic study of molecular structures of novel Schiff base derived from o-phthaldehyde and 2-aminophenol and its coordination compounds together with their biological activity. Spectrochimica Acta Part A: Molecular and Biomolecular Spectroscopy, v. 73, n. 5, p. 833-840, 2009.

ABDEL-RAHMAN, L. H. et al. Design, characterization, teratogenicity testing, antibacterial, antifungal and DNA interaction of few high spin Fe(II) Schiff base amino acid complexes. Spectrochimica Acta Part A: Molecular and Biomolecular Spectroscopy, v. 111, p. 266-276, 2013.

ADDISON, A. W. et al. Synthesis, structure, and spectroscopic properties of copper(II) compounds containing nitrogen-sulphur donor ligands; the crystal and molecular structure of aqua[1,7-bis(N-methylbenzimidazol-2[prime or minute]-yl)-2,6-dithiaheptane]copper(II) perchlorate. Journal of the Chemical Society, Dalton Transactions, n. 7, p. 1349-1356, 1984.

ADLY, O. M. I.; TAHA, A.; FAHMY, S. A. Synthesis, spectral characterization, molecular modeling and antimicrobial activity of new potentially N2O2 Schiff base complexes. Journal of Molecular Structure, v. 1054-1055, n. Supplement C, p. 239-250, 2013.

ALAGHAZ, A.-N. M. A. et al. Synthesis, spectroscopic identification, thermal, potentiometric and antibacterial activity studies of 4-amino-5-mercapto-S-triazole Schiff's base complexes. Journal of Molecular Structure, v. 1087, p. 60-67, 2015.

ARJMAND, F.; SAYEED, F.; MUDDASSIR, M. Synthesis of new chiral heterocyclic Schiff base modulated Cu(II)/Zn(II) complexes: Their comparative binding studies with CT-DNA, mononucleotides and cleavage activity. Journal of Photochemistry and Photobiology B: Biology, v. 103, n. 2, p. 166-179, 2011.

BAGIHALLI, G. B.; BADAMI, P. S.; PATIL, S. A. Synthesis, spectral characterization and in vitro biological studies of Co(II), Ni(II) and Cu(II) complexes with 1,2,4-triazole Schiff bases. Journal of Enzyme Inhibition and Medicinal Chemistry, v. 24, n. 2, p. 381-394, 2009.

BLESSING, R. H. An empirical correction for absorption anisotropy. Acta Crystallographica, Section A: Foundations of Crystallography, v. 51, p. 33-38, 1995.

CREAVEN, B. S. et al. Anticancer and antifungal activity of copper(II) complexes of quinolin-2(1H)-one-derived Schiff bases. Inorganica Chimica Acta, v. 363, n. 14, p. 4048-4058, 2010.

CRYSALISRED. Oxford Diffraction Ltda: (release 17-11-2008 CrysAlis171.NET) p. 2008.

DHAHAGANI, K. et al. Synthesis and spectral characterization of Schiff base complexes of Cu(II), Co(II), Zn(II) and VO(IV) containing 4-(4-aminophenyl)morpholine derivatives: Antimicrobial evaluation and anticancer studies. Spectrochimica Acta Part A: Molecular and Biomolecular Spectroscopy, v. 117, p. 87-94, 2014.

FARRUGIA, L. J. ORTEP-3 for windows - a version of ORTEP-III with a graphical user interface (GUI). Journal of Applied Crystallography, v. 30, n. 5, p. 565-565, 1997.

GALINI, M. et al. Structural characterization and electrochemical studies of Co(II), Zn(II), Ni(II) and Cu(II) Schiff base complexes derived from 2-((E)-(2-methoxyphenylimino)methyl)-4-bromophenol; Evaluation of antioxidant and antibacterial properties. Inorganica Chimica Acta, v. 461, p. 167-173, 2017.

GEETA, B. et al. Binuclear cobalt(II), nickel(II), copper(II) and palladium(II) complexes of a new Schiff-base as ligand: Synthesis, structural characterization, and antibacterial activity. Spectrochimica Acta Part A: Molecular and Biomolecular Spectroscopy, v. 77, n. 4, p. 911-915, 2010.

HU, X. M. et al. Synthesis, crystal structures, and antimicrobial activity of copper(II) and zinc(II) complexes derived from 2-bromo-4-chloro-6-[(2-morpholin-4-ylethylimino)methyl]phenol. Russian Journal of Coordination Chemistry, v. 42, n. 6, p. 418-422, 2016.

KACZMAREK, M. T. et al. Self-assembled synthesis, characterization and antimicrobial activity of zinc(II) salicylaldimine complexes. Inorganica Chimica Acta, v. 362, n. 9, p. 3127-3133, 2009.

KURSUNLU, A. N. et al. Synthesis, spectroscopic characterization and antimicrobial studies of Co(II), Ni(II), Cu(II) and Zn(II) complexes with Schiff bases derived from 5-bromo-salicylaldehyde. Journal of Molecular Structure, v. 1048, p. 476-481, 2013.

MACRAE, C. F. et al. Mercury: visualization and analysis of crystal structures. Journal of Applied Crystallography, v. 39, p. 453-457, 2006.

NAKAMOTO, K. Infrared and Raman Spectra of Inorganic and Coordination Compounds Part B: Applications in Coordination, Organometallic, and Bioinorganic Chemistry. 5th. New York: John Wiley & Sons Inc., 1997.

NCCLS. Reference Method for Broth Dilution Antifungal Susceptibility Testing of Yeasts. In: (Ed.). NCCLS document M27-A2. Approved Standard - Second Edition. Pennsylvania, USA: Wayne, v.22, 2002.

NCCLS. Reference Method for Dilution Antimicrobial Susceptibility Tests for Bacteria that Grow Aerobically. In: (Ed.). NCCLS document M7-A6. Pennsylvania, USA, 2003. ISBN 1-56238-486-4.

PRAKASH, A. et al. Synthesis and characterization of bioactive zinc(II) and cadmium(II) complexes with new Schiff bases derived from 4-nitrobenzaldehyde and acetophenone with ethylenediamine. Spectrochimica Acta Part A: Molecular and Biomolecular Spectroscopy, v. 76, n. 3, p. 356-362, 2010.

QIAO, X. et al. Study on potential antitumor mechanism of a novel Schiff Base copper(II) complex: Synthesis, crystal structure, DNA binding, cytotoxicity and apoptosis induction activity. Journal of Inorganic Biochemistry, v. 105, n. 5, p. 728-737, 2011.

SAKAGUCHI, S. et al. Chiral Palladium(II) Complexes Possessing a Tridentate N-Heterocyclic Carbene Amidate Alkoxide Ligand: Access to Oxygen-Bridging Dimer Structures. Angewandte Chemie International Edition, v. 47, n. 48, p. 9326-9329, 2008.

SANTOS, A. F. D. S.; OLIVEIRA, L. L. D.; MAIA, J. R. D. S. Synthesis, Characterisation and Antimicrobial Activity of Dimeric and Monomeric Copper(II)-Schiff Base Complexes IOSR Journal of Applied Chemistry (IOSR-JAC), v. 9, n. 12, p. 54-62, 2016.

SHELDRICK, G. M. SHELXL-97 - A Program for Crystal Structure Refinement: University of Goettingen, Germany 1997.

SINGH, B. K. et al. Spectroscopic, electrochemical and biological studies of the metal complexes of the Schiff base derived from pyrrole-2-carbaldehyde and ethylenediamine. Arabian Journal of Chemistry, v. 10, n. 1, p. S472-S483, 2017.

SINGH, B. K. et al. Spectroscopic characterization and biological activity of Zn(II), Cd(II), Sn(II) and Pb(II) complexes with Schiff base derived from pyrrole-2-carboxaldehyde and 2-amino phenol. Spectrochimica Acta Part A: Molecular and Biomolecular Spectroscopy, v. 76, n. 3–4, p. 376-383, 2010.

SINGH, H. L.; SINGH, J. Synthesis, spectral, 3D molecular modeling and antibacterial studies of dibutyltin (IV) Schiff base complexes derived from substituted isatin and amino acids. Natural Science, v. 04, n. 03, p. 9, 2012.

TAGHIZADEH, L. et al. New tetrahedral zinc halide Schiff base complexes: Synthesis, crystal structure, theoretical, 3D Hirshfeld surface analyses, antimicrobial and thermal studies. Materials Science and Engineering: C, v. 77, p. 229-244, 2017.

TAVMAN, A.; BOZ, I.; BIRTEKSÖZ, A. S. Spectral characterization and antimicrobial activity of 2-(5-chloro/nitro-1H-benzimidazol-2-yl)-4-bromo/nitro-phenols and their zinc(II) complexes. Spectrochimica Acta Part A: Molecular and Biomolecular Spectroscopy, v. 77, n. 1, p. 199-206, 2010.

WEN, H.-R. et al. Syntheses, structures and properties of chiral dinuclear zinc complexes with Schiff-base ligands. Inorganic Chemistry Communications, v. 20, p. 303-306, 2012.

XUE, L. W. et al. Synthesis, structures, and antimicrobial activity of nickel(II) and zinc(II) complexes with Schiff bases derived from 3-bromosalicylaldehyde. Russian Journal of Coordination Chemistry, v. 39, n. 12, p. 872-876, 2013.

XUE, L. W. et al. Synthesis, structures, and antimicrobial activity of nickel(II) and Zinc(II) complexes with 5-methoxy-2-[(3-methylaminopropylimino)methyl]phenol. Russian Journal of Coordination Chemistry, v. 37, n. 4, p. 262, 16 2011.

ZACCHINO, S. A.; GUPTA, M. P. Manual de técnicas in vitro para la deteccíon de compuestos antifúngicos. Corpus Libros Médicos y Científicos, 2007.